

# SPECTRAL INVARIANT BEHAVIOUR OF A COMPLEX 3D FOREST CANOPY

M. I. Disney<sup>a,\*</sup>, P. Lewis<sup>a</sup>

<sup>a</sup> Dept. of Geography, University College London, Gower Street, London, WC1E 6BT UK and NERC Centre for Terrestrial Carbon Dynamics - mdisney@geog.ucl.ac.uk

Commission VI, WG VI/4

**KEY WORDS:** Spectral invariant; 3D canopy structure; Monte Carlo ray tracing; recollision probability; Scots pine.

## ABSTRACT:

We present an attempt to apply the spectral invariant approach to canopy scattering of a complex forest canopy. Spectral invariant theory describes a method of expressing photon scattering as a function of purely structural properties of the canopy, the so-called photon recollision probability,  $p$  – the probability of a scattered photon undergoing further collision rather than escaping the canopy – can be used to describe the main impacts of structure on total canopy scattering. We apply a new spectral invariant formulation for canopy scattering (Lewis et al., 2007) to a detailed 3D structural model of Scots pine. This description assumes energy conservation (by definition in derivation of spectral invariant terms), and that  $p$  approaches a constant value when the scattered radiation is well-mixed (when the escape probabilities in the upward and downward direction,  $r_i$  and  $t_i$  respectively, approach each other after some finite number  $i$  of scattering interactions). We explore the behaviour of the resulting scattering from the complex models and apply the spectral invariant model description to the resulting scattering. We show that the behaviour of the spectral invariant terms ( $p$ ,  $r$ ,  $t$ ) are superficially similar to cases for simple canopies consisting of reflecting and transmitting disks, particularly for lower LAI/density cases. However, the dominance of trunks in the higher density/LAI cases violates the spectral invariant model assumptions. We suggest it may be possible to consider the scattering behaviour of the trunks and vegetation separately, considering the recollision probabilities  $p_{needle}$  and  $p_{trunk}$  independently.

## 1. INTRODUCTION

### 1.1 Canopy spectral invariants

There has been increasing interest in recent years in the so-called spectral invariant representation of vegetation canopy scattering (Knyazikhin et al., 1998; Panferov et al., 2001; Huang et al., 2007). In this approach, the total scattering from a vegetation canopy at optical wavelengths  $S_\lambda$  can be expressed as a function of wavelength  $\lambda$  as follows:

$$S_\lambda = t_0 + (1 - t_0) \sum_{i=1}^{i=\infty} s_i \omega_\lambda^i \quad (1)$$

where  $t_0$  is the probability of radiation being transmitted through the canopy without interacting with canopy elements (the zero-order transmittance),  $\omega$  is the canopy element single scattering albedo and the terms  $s_i$  are spectrally-invariant terms dependent on the incident radiation distribution, the arrangement and angular distribution of canopy elements, and the ratio  $\zeta_\lambda$  of leaf transmittance  $T_{leaf,\lambda}$  to total leaf scattering ( $\omega_{leaf,\lambda} = T_{leaf,\lambda} + R_{leaf,\lambda}$ ) where  $R_{leaf,\lambda}$  is the leaf spectral reflectance i.e.

$$\zeta_\lambda = T_{leaf,\lambda} / (R_{leaf,\lambda} + T_{leaf,\lambda}) \quad (2)$$

The canopy spectral transmittance  $T_{bs,\lambda}$  reflectance  $R_{bs,\lambda}$  and absorptance  $A_{bs,\lambda}$  for a canopy with a totally absorbing lower boundary ('black soil') can be expressed in similar forms. Relationships between the spectral invariant terms in  $S_\lambda$ ,  $T_{bs,\lambda}$ ,  $R_{bs,\lambda}$  and  $A_{bs,\lambda}$  can be expressed using the concept of a

recollision probability  $p_i$  (the probability that radiation incident on leaves after  $i$  interactions recollide with other canopy elements rather than escaping from the canopy). This recollision probability can also be considered in terms of the corresponding 'escape' probabilities in the upward and downward directions respectively  $r_i$  and  $t_i$  i.e.  $p_i + r_i + t_i = 1$  for energy conservation.

There have been various treatments of the concept of spectral invariants, notably by Knyazikhin et al. (1998) and Panferov et al. (2001) who have shown that the recollision probability is in fact the principal eigenvalue of the radiative transfer operator. Disney and Lewis (1998) independently noted that the multiple scattered radiation from a 3D barley canopy was well-behaved after relatively few scattering interactions. In both cases, the multiple scattering can be phrased as an infinite sum of scattering terms (a Neumann series). This sum represents the multiple interactions (and attenuation) of scattered radiation. This description of canopy scattering is spectrally invariant, depending on structure alone. The spectral invariant approach has been used by Smolander and Stenberg (2005) and others to represent scattering at multiple scales including the leaf (Lewis and Disney, 2007), shoot (Smolander and Stenberg, 2005; Mottus et al., 2007).

As noted by Huang et al. (2007) and others, the recollision probability tends to converge to its final value after relatively few iterations. can be considered the recollision probability of the radiation in the canopy when it is 'well mixed' (i.e. it has settled down to a stable value). 'Well-mixed' can be considered the point at which the escape probabilities in the upward and downward direction  $r_i + t_i$  are effectively equal.

---

\* Corresponding author.

There are two primary reasons why the spectral invariant approach to describing canopy scattering is attractive. Firstly, such a representation can provide a rapid, structurally consistent way to model canopy scattering. This potentially makes the spectral invariant description very useful in applications where rapid, consistent models of scattering are required, such as in look-up-table (LUT) retrieval of biophysical parameters from observations of scattering, or for assimilation of observations into models of ecosystem function. Speed is a pre-requisite in both these applications; a consistent (across wavelength and canopy structure) representation of scattering is highly desirable and makes analysis much more straightforward as only a single model of scattering is required..

Secondly, the spectral invariant approach permits the separation of scattering behaviour due to structural and biochemical influences (Lewis and Disney, 2007). These properties are often coupled and so separation of their behaviour may permit retrieval of either alone. Without this separation such retrieval may not be possible.

This paper presents an exploration of the spectral invariant approach to describing scattering from a highly-detailed 3D Scots pine canopy.

## 2. MATERIALS AND METHODS

### 2.1 3D structural model

A 3D structural model of Scots pine was developed using the Treegrow/PINOGRAM model of Leersnijder (1992). The model is based on measurements of canopy structural development made in the field. Scots pine stands were simulated over a range of ages (5 to 50 years in 5 year steps) and densities. Tree spacing was varied between ~1.5m and ~6m, covering the observed range of densities for such a canopy in managed forest stands in the UK. Full details of stand development and comparison to observed data are given in Disney et al. (2006). It is shown that the resulting canopies can be used to simulate observed reflectance well.

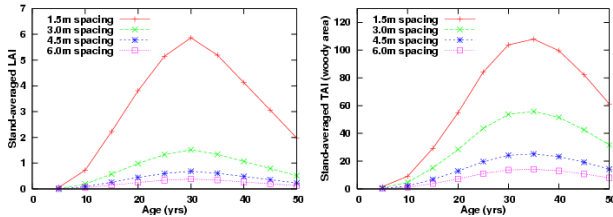


Figure 1. Stand-averaged LAI and woody area with age and density.

Figure 1 shows the variation of the stand properties with age and density. It can be seen that the stand-averaged LAI increases with age to a maximum at age 30 years. The equivalent measure of trunk area trunk, ‘trunk area index’, varies in the same manner, but peaks slightly later at around age 35 years due to the shift to proportionately reduced leaf area (increased trunk area) at increased age.

Figure 2 shows examples of the variation in tree spacing and crown shape (for Sitka spruce in this case) are typically observed in managed tree stands of the sort being modelled. As the trees develop in close proximity to one another, the crown size reduces and the stands become dominated internally by large quantities of trunk area.



Figure 2. Managed forest stands of 15 years (left) and 35 years (right).

### 2.2 Canopy simulation and modelling

To examine the spectral invariant behaviour of the Scots pine canopy, energy conservative (totally scattering/absorbing) simulations were carried out using the Monte Carlo ray tracing (MCRT) model, *drat* (see Pinty et al., 2004 and Widlowski et al., 2007 for model intercomparison). All 7 combinations of  $p_{leaf, trunk, soil} = 0, 1$  were simulated. In order to simulate the zero order transmission component ( $t_0$  from equation 1), reflectance and was simulated in a case with no soil i.e. illuminated from above, but with transmitted radiation passing directly through the lower boundary. In all cases, scattering was simulated to scattering order 100. This might seem excessive but when considering the scattering in energy conservative cases (no absorption), the amount of energy remaining after many scattering interactions can still be significant. The implications for this become apparent below.

Analysis of the resulting scattering behaviour is presented below, as well as results from attempting to fit the model representation of Lewis et al. (2007). This model describes R, T, S as follows:

$$R_{bs,\lambda} = \frac{1}{2}(1-t_0)(1-p_\infty) \left[ \frac{\omega_\lambda}{1-p_\infty\omega_\lambda} + \frac{c_1 d_1 \omega_\lambda}{1-p_\infty d_1 \omega_\lambda} \right] \quad (3)$$

$$T_{bs,\lambda} = t_0 + \frac{1}{2}(1-t_0)(1-p_\infty) \left[ \frac{\omega_\lambda}{1-p_\infty\omega_\lambda} - \frac{c_2 d_2 \omega_\lambda}{1-p_\infty d_2 \omega_\lambda} \right] \quad (4)$$

$$\frac{(S_{bs,\lambda} - t_0)}{(1-t_0)} = \frac{(1-p_\infty)\omega_\lambda}{1-p_\infty\omega_\lambda} + \frac{(1-p_\infty)}{2} \left[ \frac{c_1 d_1 \omega_\lambda}{1-p_\infty d_1 \omega_\lambda} - \frac{c_2 d_2 \omega_\lambda}{1-p_\infty d_2 \omega_\lambda} \right] \quad (5)$$

where, under energy conservation

$$\frac{c_1 d_1}{1-p_\infty d_1} = \frac{c_2 d_2}{1-p_\infty d_2} \quad (6)$$

The terms  $c_{1,2}$  and  $d_{1,2}$  are ‘fitting’ (i.e. not biophysical) parameters parameter. The derivation of the above model and assumptions underlying it are described in Lewis et al. (2007). The key for this analysis is that the behaviour of the escape probabilities  $r_i$ ,  $t_i$  in the upward and downward directions respectively are assumed well-behaved i.e. that  $\sqrt{r_i t_i}$  is approximately constant once  $p_\infty$  has been reached.

### 3. RESULTS

#### 3.1 Scattering behaviour

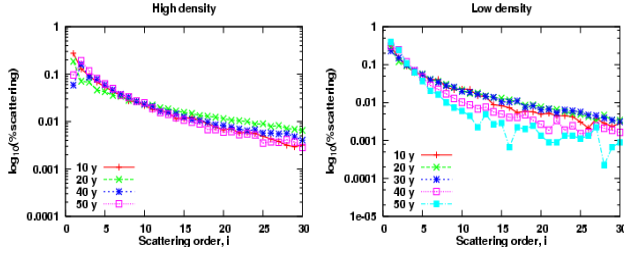


Figure 3. Canopy scattering behaviour as a function of scattering order,  $i$ .

Figure 3 shows the decay of total diffuse scattering (%) for high density (average tree spacing  $< 2\text{m}$ ) and low density (average tree spacing  $> 5\text{m}$ ) cases, as a function of scattering order,  $i$ . The terms ‘high/low density’ are used to imply the same spacing through the following text. In log space, the scattering in both cases decreases relatively rapidly for the first few scattering orders and then much more gradually with increasing  $i$ . In the high density case, two things become apparent: i) there is little difference between behaviour for different ages, except over the first two scattering orders; ii) the first order behaviour can be unexpected, with greater scattering at  $i=2$  than  $i=1$  in some cases. In the low density stands, there is separation of the scattering behaviour between the different stand ages. Also apparent is that simulations become quite noisy even at scattering orders  $< 20$ .

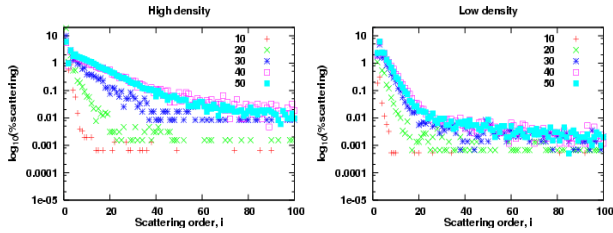


Figure 4. Canopy scattering behaviour as a function of scattering order,  $i$  density and age.

Figure 4 shows the same results as in figure 3, but over all scattering orders (i.e. to  $i=100$ ). As  $i$  exceeds 30 we see that the separation of scattering behaviour with stand age becomes more apparent even in the high density case. Most importantly, we see that the *rate of decay* of scattering is still decreasing for the older canopies and does not seem to have settled down to a constant rate, even at  $i=100$ . This is important as the model fitting described below assumes constant recollision probability  $p_\infty$  i.e. when the rate of decay of scattering from  $i$  to  $i+1$  is constant.

In the low density case, conversely, the scattering behaviour has two distinct phases. The first settles down quickly to a constant (steep) decay; the second then takes over at  $i=10-30$  (depending on stand age) and has a much more gradual decay.

#### 3.2 Escape probabilities $r_i$ , $t_i$

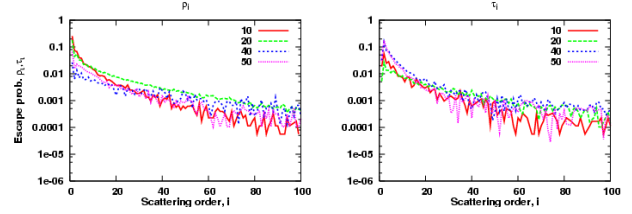


Figure 5. Upward and downward escape probabilities ( $r_i$ ,  $t_i$ ) for a high density canopy (2-3m tree spacing).

Figure 5 shows the behaviour of the escape probabilities in the upward ( $r_i$ ) and downward ( $t_i$ ) directions for the high density canopy as function of  $i$ . In both cases the behaviour follows the same path. This differs distinctly from the cases observed in idealised disk canopies seen in Lewis et al. (2007), where as  $r_i$  decreases,  $t_i$  increases. Figure 6 shows the same information for the low density canopy case.

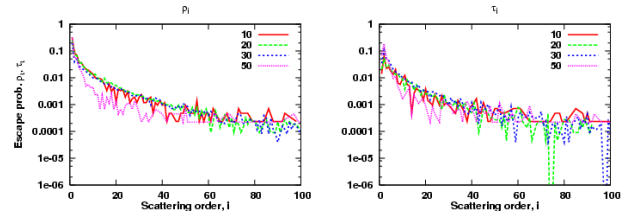


Figure 6. Upward and downward escape probabilities ( $r_i$ ,  $t_i$ ) for a low density canopy (5-6m tree spacing).

#### 3.3 Recollision probability, $p$

Figure 7 shows the variation of recollision probability  $p_i$  ( $1 - r_i - t_i$ ) as a function scattering order for high and low density stands (upper/lower panels) and for two ages, 10 and 45 years (left/right panels). In each case,  $p_i$  is shown for three view zenith angles,  $0^\circ$ ,  $30^\circ$  and  $60^\circ$  (sun zenith is  $0^\circ$  in all cases).

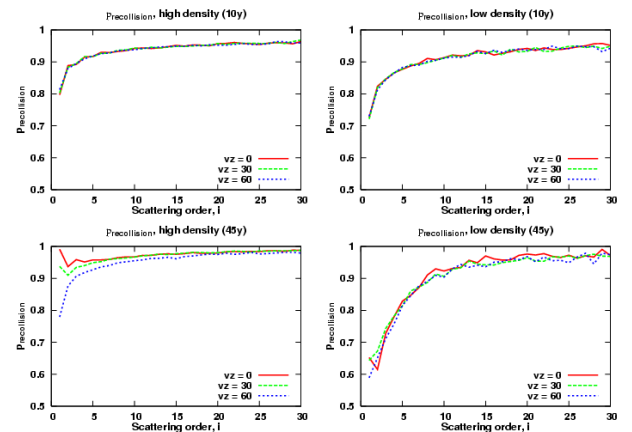


Figure 7. Recollision probability,  $p_i$ , as a function of age, scattering order and view zenith angle.

The recollision probability varies in a similar way to that seen by Lewis et al. (2007) for idealised disk canopies. Values start between 0.6 and 0.8 for  $i=1$  and progress to  $> 0.9$ . In all cases in figure 7,  $p$  does not appear have reached  $p_\infty$  even at  $i=30$ . There

is little variation with view zenith in the high density case, but this is not true for the lower density case. Other, different behaviour is seen for high density case at low  $i$ , where  $p$  can reduce before increasing again.

### 3.4 Model fitting

Figure 8 shows the results of fitting the model of spectral invariants presented by Lewis et al. (2007) (equations 3-5) to the simulated values of canopy reflectance shown above. Figure 9 shows the same information for the low density stand. In each case the solid lines are the model fits and the symbols the corresponding MCRT-simulated values.

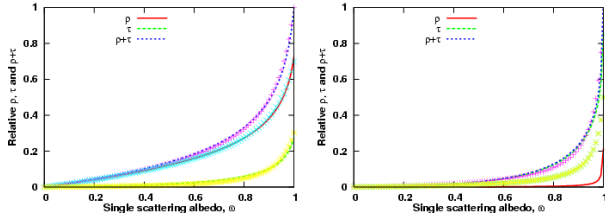


Figure 8. Model fit for high density stand, age 10yrs (left) and 45yrs (right)

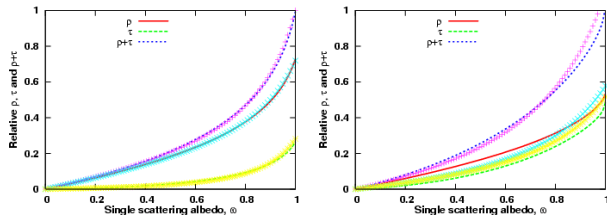


Figure 9. Model fit for low density stand, age 10yrs (left) and 45yrs (right).

The model fitting results are presented as a function of needle single scattering albedo,  $\omega$ . As a result of fitting the spectral invariant model (equations 3-5) we can express canopy scattering in this way over the whole range of possible values of  $\omega$ , rather than for some specific value. This is one of the advantages of using spectral invariants: scattering behaviour is expressed purely a function of the structural terms contained within the model, rather than as some combined structural-biochemical scattering behaviour at specific wavelengths.

## 4. DISCUSSION

The scattering behaviour of the 3D Scots pine canopy shown in figures 3 and 4 is superficially similar to that shown by Lewis et al. (2007) for idealised disk canopies i.e. rapid reduction of scattering in the first two orders, followed by a gradual reduction until a point is reached at which further reduction of scattering is constant (in log space). This is the point at which the scattering can be considered ‘well-mixed’ and that  $p = p_\infty$ . Lewis et al. (2007) note that this typically occurs at  $i \cong 2LAI$ .

However, closer inspection reveals some significantly different behaviour. In particular, the first orders of scattering can increase, particularly for the very dense stands. In addition, there are large differences in behaviour with age: for the older, larger trees in figure 4 the scattering is clearly still levelling out and has not reached the plateau of  $p = p_\infty$ , even after 100

scattering interactions. This is largely due to the domination of the high density/age stands of the trunk material. Figures 1 and 2 show how much trunk material can be contained within a scene. In the energy conservation case, this trunk material is white, and so the scenes are dominated by large areas of totally reflecting solid objects (no transmission). This appears to have significant implications for the model representation and fitting.

We note that in the low density case, there appear to be two separate decay processes occurring. The first, due to the needles, dominates scattering orders  $< 20$  causing a rapid decay. Beyond this, a second decay rate takes over which is far more gradual. This is likely to be the influence of the trunks. Once a photon has penetrated through the upper crown layer, it can interact many times with the trunks before escaping through the upper (or lower) boundary. This behaviour tends to dominate for the denser/older canopies and will result in there being effectively two values of  $p$ ,  $p_{needle}$  and  $p_{trunk}$ .

The results of fitting the spectral invariant model described by Lewis et al. (2007) appear to be reasonable, particularly for the younger trees and lower density stands. However, for the high density/age the model form is clearly not appropriate. Figure 10 illustrates what is occurring during the model fitting.

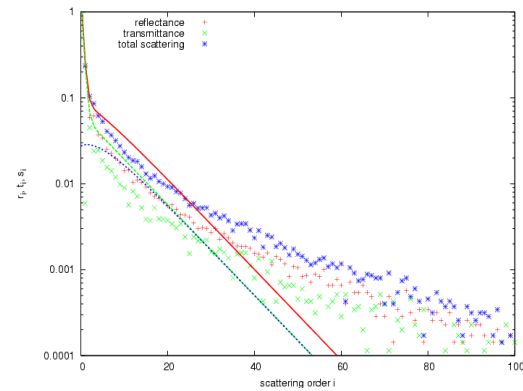


Figure 10. Model fit with scattering order,  $i$ .

Figure 10 shows the decay of the MCRT-simulated scattering terms, as well as the modelled versions of these terms resulting from fitting equations 3-5 to the simulated scattering. Although the model *can* fit to the first few scattering orders, where total energy is large, the decay of the modelled terms is far steeper than observed. As a result, the modelled value of  $p$  departs quite strongly from the ‘actual’ value, as a result of the two-stage behaviour described above. The result of this inappropriate fit is that although the model may seem to fit quite well, it is doing so for the wrong reasons.

A second issue that can be seen in figure 10 is the behaviour of the separate scattering components. The form of the spectral invariant model outlined above assumes energy conservation, that  $r_i, t_i$  the upward and downward escape probabilities, approach a constant value and that  $\sqrt{r_i t_i}$  is approximately constant once  $p_\infty$  has been reached. This is clearly not the observed behaviour in figure 6. As a result, the final spectral invariant model is not appropriate for the 3D Scots pine canopies simulated here.

A further departure from the assumptions of the spectral invariant model is the issue of energy conservation. In the most extreme high density/age case, there can be energy of the order of 0.05 to 0.5% remaining even at  $i=100$ . As a result, the

assumption of energy conservation is not met. Although this might appear to be a very small amount of energy, it is the rate of decay at this stage which determines  $p_\infty$ .

As a result of these departures, and the lack of model fit for higher orders of scattering, we suggest that the scattering from the trunks and needles may need to be treated separately, requiring the formulation of the spectral invariant model for scattering from needles/soil (via  $p_{needle}$ ) and trunks/soil (via  $p_{trunk}$ ) as well as multiple scattering between the two components (via combination of  $p_{needle}$  and  $p_{trunk}$ ). This approach was used in Saich et al. (2004). In this case, canopy scattering,  $\rho$ , was expressed in the form

$$\rho = W + WS + T + TS + WT \quad (6)$$

Where W is the scattering from needles only; WS is scattering from needles and soil; T is scattering from trunk only; TS, scattering between trunk and soil; and WT is scattering between needles and trunk. Each of the terms in equation (6) was represented through an expression of the form

$$\rho_{w,t,s} \propto \frac{a\omega}{1-b\omega} \quad (7)$$

from the Neumann series solution for multiple scattered components. In the case of Saich et al. (2003), a and b were considered ‘empirical’ model fitting coefficients. However it is clear that  $a \propto (1-p)$  and  $b \propto p$  in terms of the form expressed in equations (3-5). This approach worked extremely well, and was able to describe observed scattering very closely. However the model was essentially a semi-empirical one: the various scattering terms introduced in the form of equation (6) having no direct physical equivalent.

## 5. CONCLUSIONS

A spectral invariant approach to modelling canopy scattering in a complex 3D Scots pine canopy was explored. Total canopy scattering was simulated for a range of structural scenarios spanning the range of observed canopies, using a Monte Carlo ray tracing model. A model of scattering phrased in terms of spectral invariant terms developed for an idealised disk canopy (Lewis et al., 2007) was applied to the resulting modelled scattering. The spectral invariant approach considers canopy scattering in energy conservation cases (totally scattering/absorbing canopy/soil components).

While the scattering behaviour of the Scots pine canopies superficially resembled that from the idealised disk cases, scattering decayed much more slowly. In addition, the more dense the canopy, the less the scattering behaviour resembled that of the disk canopies. Some significant radiation is

The behaviour of  $p$ , the recollision probability, was similar to that observed for the idealised disk canopies. However, the behaviour of  $r_i$  and  $t_i$ , the upward and downward escape probabilities was somewhat different. In particular, assumptions regarding the behaviour of these terms in the spectral invariant model were not met.

The spectral invariant model appears to fit quite well to the MCRT-modelled scattering behaviour. However, closer inspection shows that although the model might provide a quite

close fit in some cases (particularly for lower density/age stands), this is for the wrong reasons. The model form is not appropriate for the observed scattering behaviour.

It is proposed that the presence of large areas of trunk within the canopy dominate the scattering response, particularly at higher orders of scattering. Given the total area of trunk and branch can approach 100m<sup>2</sup> per m<sup>2</sup> of ground area in extreme cases, this is not surprising.

It is proposed that a spectral invariant model for this type of canopy requires a more complex representation to cope with: non-transmitting needles; three components as opposed to two which greatly increases the number of scattering components in the resulting signal. Specifically, observed scattering suggests the application of separate recollision probabilities for the trunk/branch and needle components,  $p_{needle}$  and  $p_{trunk}$ .

The extreme density simulations carried out here are not realistic in that intersection of scattering elements cannot be precluded for tree spacing < ~3m. In addition, the large areas of trunk and branch render the needle scattering far less significant as a proportion of total scattering.

Future work will include simulation of canopies of intermediate structural complexity i.e. somewhere between the idealised disk cases and the 3D Scots pine canopies seen here. Examples of these would be heterogeneous broadleaf-type canopies which have trunk material, but not in such large quantities as for the Scots pine canopies. The conifer-like and birch-like scenes of third RAMI experiment will provide examples for this (Widlowski et al., 2007).

## ACKNOWLEDGEMENTS

We gratefully acknowledge support from the University College London Research Computing Facilities through access to the Central Computing Cluster (C<sup>3</sup>) for much of the computing for this work. Some of this work was funded by the Natural Environment Research Council through the Centre for Terrestrial Carbon Dynamics (CTCD). The authors also gratefully acknowledge fruitful discussions with Yuri Knyazikhin and colleagues on the subject of spectral invariants.

## REFERENCES

- Disney, M. I. and Lewis, P. (1998) Multiple scattering behaviour of a 3D barley canopy, *in proc. IGARSS98*, Seattle, USA.
- Disney, M. I., Saich, P., and Lewis, P. (2003). Modelling the radiometric response of a dynamic, 3D structural model of Scots Pine in the optical and microwave domains, in *Proceedings of IEEE Geoscience and Remote Sensing Symposium IGARSS'03*, **6**, 3537–3539.
- Disney, M. I., Lewis, P., Quaife, T. and Nichol, C. (2005). A spectral invariant approach to modelling canopy and leaf scattering, in *Proceedings of ISPMSRS'05, Beijing, China, October 17-19 2005*, ISSN 1682-1750, 318–320.
- Disney, M. I., Lewis, P. and Saich, P. (2006). 3D modelling of forest canopy structure for remote sensing simulations in the optical and microwave domains, *Rem. Sens. Environ.*, **100**(1), 114–132.
- Disney, M. I., Lewis, P. and Saich, P. (2006). 3D modelling of

forest canopy structure for remote sensing simulations in the optical and microwave domains, *Rem. Sens. Environ.*, **100**(1), 114–132.

Knyazikhin, Y., Kranigk, J. V., Myneni, R. B., Panferov, O. and Gravenhorst, G., (1998). Influence of small-scale structure on radiative transfer and photosynthesis in vegetation cover, *Journal of Geophysical Research*, **103**, 6133–6144.

Leersnijder, R. P. (1992) PINOGRAM: A Pine Growth Area Model, PhD thesis Wageningen University.

Lewis, P. and Disney, M. I. (2007) Spectral invariants and scattering across multiple scales from within-leaf to canopy, *Rem. Sens. Environ.*, doi:10.1016/j.rse.2006.12.015

Lewis, P., Disney, M. I., Knyazikhin, Y., Quaife, T. and Schull, M. (2007) Modelling canopy reflectance with spectral invariants, in *proc. ISPMRS07*, Davos, March 11-15 2007.

Panferov, O., Knyazikhin, Y., Myneni, R. B., Szarzynski, J., Engwald, S., Schnitzler, K. G. and Gravenhorst, G. (2001). The role of canopy structure in the spectral variation of transmission and absorption of solar radiation in vegetation canopies, *IEEE Trans. Geosci. Rem. Sens.*, **39**(2), 241–253.

Pinty, B., Widlowski, J.-L., Taberner, M., Gobron, N., Verstraete, M. M., Disney, M. I., Gascon, F., Gastellu, J.-P., Jiang, L., Kuusk, A., Lewis, P., Li, X., Ni-Meister, W., Nilson, T., North, P., Qin, W., Su, L., Tang, S., Thompson, R., Verhoef, W., Wang, H., Wang, J., Yan, G., Zang, H. (2004). Radiation Transfer Model Intercomparison (RAMI) exercise: Results from the second phase, *Journal of Geophysical Research*, **109**, D06210, doi:10.1029/2003JD004252.

Saich, P., P. Lewis, M. Disney, P. van Oevelen, I. Woodhouse, B. Andrieu, C. Fournier, S. Ljutovac (2004) Development of vegetation architectural models for remote sensing Applications, final report of ESA Contract 14940.

Smolander, S., and Stenberg, P. (2005). Simple parameterizations of the radiation budget of uniform broadleaved and coniferous canopies, *Rem. Sens. Environ.*, **94**, 355–363.

Widlowski, J.-L., Taberner, M., Pinty, B., Bruniquel, V., Disney, M. I., Fernandes, R., Gastellu-Etchegorry, J. P., Gobron, N., Kuusk, N., Lavergne, T., Leblanc, S., Lewis, P., Martin, E., Mottus, M., North, P. R. J., Qin, W., Robustelli, M., Rochdi, N., Ruiloba, R., Soler, C., Thompson, R., Verhoef, W., Verstraete, M. M. and Xie, D. (in press). The third Radiation transfer Model Intercomparison (RAMI) exercise: Documenting progress in canopy reflectance models, *Journal of Geophysical Research (Atmospheres)*.